PHOTOSYNTHETICA
International Journal for Photosynthesis Research

DOI 10.32615/ps.2022.047 PHOTOSYNTHETICA 61 (SI): 190-202, 2023

Special issue on Recent advances in photomodulation in higher plants, algae, and bryophytes

Changes in the photosynthetic performance, the activity of enzymes of nitrogen metabolism, and proline content in the leaves of wheat plants after exposure to low CO_2 concentration

A. IVANOV[*,+], A. KOSOBRYUKHOV[*], V. KRESLAVSKI[*], and S.I. ALLAKHVERDIEV[*,**,***,#,+]

Institute of Basic Biological Problems, Russian Academy of Sciences, Institutskaya Street 2, Pushchino, 142290 Moscow Region, Russia[*]
K.A. Timiryazev Institute of Plant Physiology, Russian Academy of Sciences, Botanicheskaya Street 35, 127276 Moscow, Russia[**]
Faculty of Science, King Abdulaziz University, 21589 Jeddah, Saudi Arabia[***]
Faculty of Engineering and Natural Sciences, Bahcesehir University, Istanbul, Turkey[#]

Abstract

The changes in photosynthetic activity, as well as the activity of nitrogen-metabolism enzymes, the intensity of lipid peroxidation, and proline content were studied in *Triticum aestivum* L. plants after their incubation at a low CO_2 concentration in a sealed chamber for 10 d. CO_2 deficiency ($-CO_2$) compared to normal CO_2 concentration (control) led to a decrease in the rate of O_2 gas exchange at the plateau of the light curve and quantum yield of photosynthesis. The maximum and effective quantum photochemical yields also decreased. CO_2 deficiency reduced the activity of nitrate reductase, but increased the activities of nitrite reductase, glutamine synthetase, and glutamate dehydrogenase, and promoted proline accumulation. It is assumed that with a lack of CO_2, an excess of nitrogen-containing compounds occurs, which must be removed from metabolic processes. Also, we suggest the partial storage of nitrogen in the form of nitrogen-containing compounds such as proline.

Keywords: chlorophyll fluorescence; growth; low CO_2; nitrogen cycle; photosynthetic activity.

Introduction

Many works are studying the impact of the increase in atmospheric CO_2 observed in nature in recent decades on various physiological processes in plant leaves (Terashima *et al.* 2014). On the other hand, CO_2 deficiency can be observed in plants due to stomatal closure in the process of adaptation to abiotic stresses, which leads to C/N

Highlights

- The deficiency of CO_2 decreases PSII activity and activity of the nitrate reductase
- Low CO_2 reduced the activity of nitrate reductase and induced proline accumulation
- Reducing CO_2 increased the activities of nitrite reductase and glutamine synthase

Received 5 October 2022
Accepted 11 November 2022
Published online 1 December 2022

[+]Corresponding author
e-mail: demfarm@mail.ru (A. Ivanov)
suleyman.allakhverdiev@gmail.com
(S.I. Allakhverdiev)

Abbreviations: Fd – ferredoxin; Gln – glutamine; Glu – glutamate; GOGAT – glutamate synthase; GS – glutamine synthetase; MDA – malondialdehyde; NAD-GDH – glutamate dehydrogenase; NiR – nitrite reductase; NR – nitrate reductase; Pro – proline; ProDH – proline dehydrogenase.

Acknowledgments: The work was financially supported by the Ministry of Science and Higher Education of the Russian Federation (No. 122041100071-1) and with partial financial support from the Russian Foundation for Basic Research (No. 21-54-53015). SIA was supported by a grant from the Russian Science Foundation (No. 19-14-00118). Fig. 3 was supported by a state assignment from the Ministry of Science and Higher Education of the Russian Federation (No. 122050400128-1). The authors thank Pavel Pashkovskiy for assisting with the writing.
Conflict of interest: The authors declare that they have no conflict of interest.

imbalance (Ye *et al.* 2022). Note that low concentrations of CO_2 can occur in nature, not only due to the closure of stomata but also in thickened crops and greenhouses with a large number of plants. However, the plant response to low CO_2 concentration at the physiological and biochemical levels is still insufficiently studied (Wu *et al*. 2020). It has been shown that the oxygen evolution rate remains at a fairly high level, despite a decrease in CO_2 concentration in the intercellular spaces of leaves (Ivanov 2015). On the one hand, under these conditions, there is a change in the ratio of carboxylase and oxygenase activities of ribulose bisphosphate carboxylase/oxygenase (EC 4.1.1.39) and an increase in the photorespiration rate. In this case, the reduced ferredoxins of the photosynthetic electron transport chain can serve as an electron donor in the reactions of reassimilation of ammonia released during photorespiration in C_3 plants through the glutamate synthase cycle (Miflin and Habash 2002). On the other hand, in addition to the main function as a source of electrons in processes of CO_2 fixation, ferredoxins (Fd) can participate in the primary assimilation of nitrogen by reducing NO_2^-, which acts as an alternative electron acceptor (Noctor and Foyer 1998).

The main source of nitrogen for the plant is nitrates and ammonium (Ye *et al.* 2022). The nitrogen cycle includes both the uptake of nitrates from the soil and the hydrolysis of storage N-compounds, as well as the reassimilation of ammonia released during photorespiration (Miflin and Habash 2002). Nitrates absorbed from the soil using NO_3^- transporters are reduced to ammonium in sequential reactions using nitrate reductase (NR, EC 1.6.6.1) in the cytosol and nitrite reductase (NiR, EC 1.6.6.4) in plastids/chloroplasts. Ammonium is first converted by glutamine synthetase to glutamine (Gln) (GS1 in the cytosol and GS2 in chloroplasts, EC 6.3.1.2), which is then converted to glutamate (Glu) by glutamate synthase (Fd-GOGAT [EC 1.4.7.1] in chloroplasts and NADH-GOGAT [EC 1.4.1.14] in plastids) (Ireland and Lea 1999, Ziegler *et al.* 2003, Robredo *et al.* 2011).

The combined action of GS and GOGAT is the main pathway for the assimilation of ammonia. Gln and Glu play an important role in the synthesis of other amino acids, as well as practically all nitrogen compounds in plant cells (Ziegler *et al.* 2003). On the other hand, ammonium may be directly incorporated into Glu in amination reactions involving glutamate dehydrogenase (NADH-GDH, EC 1.4.1.2), especially at high NH_4^+ concentrations, but the function of this enzyme is a subject of debate (Ireland and Lea 1999, Ziegler *et al.* 2003). Since GDH reversibly deaminates Glu (NAD-GDH), the physiological role of this enzyme *in vivo* is likely, obtaining 2-oxoglutarate and reducing equivalents for use in other metabolic processes (Robredo *et al.* 2011).

Optimal functioning and coordination of carbon and nitrogen metabolism play a key role in plant life. Photosynthetic carbon pathway reactions provide available energy for NO_3^- reduction and C-skeletons for subsequent amino acid synthesis. With an increased content of carbohydrates in plant leaves, an increase in the activity of enzymes associated with N metabolism may occur (Zhang *et al.* 2011), contributing to the reassimilation of NH_4^+ produced during photorespiration. This process may also be a consequence of light induction of glutamate synthesis (Kendall *et al.* 1986, Ferrario-Méry *et al.* 2002) and gene expression of several N-pathway enzymes (Lam *et al.* 1996). Thus, there are many points of mutual control of carbon and nitrogen metabolism at the level of gene expression and regulation of enzyme activity (Commichau *et al.* 2006).

In addition, both nitrogen and carbon pathways use the same reducing equivalents and some of the intermediates obtained in the primary photochemical processes. This competition becomes especially noticeable when one of these metabolic pathways is limited, for example, when CO_2 assimilation decreases under stress conditions (Sánchez-Rodríguez *et al.* 2011). A relationship between NO_3^-/NH_4^+ and abiotic stress responses in plants, focusing on stresses from nutrient deficiencies, unfavorable pH, ions, and drought, which can lead to C/N imbalance, is considered in the review of Ye *et al.* (2022).

Mutual regulation of C and N metabolism occurs already at the level of primary assimilation of CO_2 and NO_2^- with the participation of ferredoxin, which is a component of the electron transport chain of chloroplasts PSI and carries out the reduction of inorganic molecules (Eichelmann *et al.* 2011). Transfer of 4 electrons (to 2 $NADP^+$) together with 12 H^+ during linear electron transport from H_2O to $NADP^+$ leads to the formation of three ATP molecules, which are enough to assimilate one CO_2 molecule in the Calvin cycle. An additional amount of ATP can be formed by transferring electrons to alternative acceptors with the inclusion of metabolic pathways with a lower ATP consumption per electron (Eichelmann *et al.* 2011). NO_2^- can act as an alternative electron acceptor, the reduction of which leads to the formation of additional ATP in the case of limiting the CO_2 absorption (Noctor and Foyer 1998).

Under unfavorable environmental conditions, the accumulation of proline (Pro) is often observed in plant leaves, the synthesis of which is most often explained by the activation of specific biochemical mechanisms to counteract the harmful effects of stress. We have previously shown that there is a direct correlation between the change in stomatal conductance and the formation of Pro in the leaves of wheat plants (Ivanov 2015). A decrease in CO_2 fixation due to stomatal closure under stress conditions also leads to the C/N imbalance and the accumulation of excessive amounts of nitrogen-containing substances, for example, Pro. However, little attention has been paid to the study of the impact of CO_2 deficiency on photosynthetic processes and nitrogen metabolism in plant cells. Therefore, the purpose of this study was to study the changes in photosynthetic activity, the activity of key enzymes of N metabolism, and the accumulation of Pro in wheat leaves grown at reduced CO_2 content in the environment.

Materials and methods

Plant material and growing conditions: Wheat plants (*Triticum aestivum* L.) were used as the object of research, the seeds of which were germinated in 0.5-L vessels.

As a substrate, we used river sand with a nutrient solution containing 3.9 mM KNO_3, 3 mM $Ca(NO_3)_2$, 0.7 mM $MgSO_4$, 0.05 mM $Mg(NO_3)_2$, 1.1 mM KH_2PO_4, and trace elements 24 μM H_3BO_3, 4.5 μM $MnSO_4$, 3.5 μM $ZnSO_4$, 1 μM $CuSO_4$, 1 μM $CoSO_4$, 0.28 μM Na_2MoO_4, and 1.4 μM Fe–EDTA (Coic and Lesaint 1971). Plants were grown under controlled conditions under white fluorescent lamps at 12-h photoperiod, the temperature of 24/20°C (day/night), relative air humidity of 70–80%, and photon flux density of 400 ± 24 μmol(photon) m^{-2} s^{-1}. Watering was carried out daily with distilled water until the substrate was completely saturated. Watering the plants in the incubation chamber at low CO_2 was carried out using a special valve system.

Some of the vessels with 10-d-old wheat seedlings were placed in a sealed plexiglas chamber (*Percival*, *Model PT-80*, Boone, IA) with a volume of 13.6 L, where, as a result of natural absorption by plants, the concentration of CO_2 in the air decreased from 436 to 48 ppm (compensation point) after 3 d from the start of incubation, which was monitored using the compact CO_2 gas analyzer (*LI-850*, *LI-COR Biosciences*, USA). After 10 d of incubation of plants under low CO_2 concentration, the chamber was opened and plant parameters were monitored for the next 2 d at natural CO_2 concentration.

During the experiment, the parameters of photosynthesis and the activity of nitrogen-metabolism enzymes of the 2nd leaf of plants were measured immediately after opening the plant incubation chamber at a low concentration of CO_2 ($-CO_2$) and for the next 2 d under conditions of normal concentration of CO_2. In parallel, similar measurements were carried out in the plants constantly growing at natural CO_2 concentration (control).

Growth parameters were determined by the dry biomass of the old (1st leaf), younger (2nd leaf), and 3rd leaves throughout the entire growing period, except for the period when the plants were in the incubation chamber. To determine dry biomass, fresh leaves were placed in a thermostat for 3 d at 80°C.

Chl *a* fluorescence: The induction curves of leaf Chl *a* fluorescence were recorded by fluorimeter (*Heinz Walz*, Germany). The measurements were carried out immediately after the opening of the chamber, in which the plants were incubated at a low concentration of CO_2, and also during the next 2 d at a natural CO_2 concentration. The levels of minimum (F_o) and maximum (F_m) fluorescence were determined after 15-min exposure to leaves in the dark. The PSII maximal quantum yield was determined using the formula $F_v/F_m = (F_m - F_o)/F_m$ (Goltsev *et al.* 2016).

The light was switched for 10 min [I = 190 μmol(photon) m^{-2} s^{-1} PAR]. The intensity used was close to the PAR incident on plants. The intensity of the saturating light was 6,000 μmol(photon) m^{-2} s^{-1}. Saturating pulses were generated every 30 s. The effective quantum yield of PSII (Y_{II}) in leaves adapted to light exposure was calculated by the formula: $Y_{(II)} = (F_m' - F')/F_m'$. The values of the coefficients of nonphotochemical quenching of fluorescence of Chl *a* (NPQ and q_N) were determined using the formula: $NPQ = (F_m - F_m')/F_m'$ and $q_N = (F_m - F_m')/F_v$. The relative rate of PSII electron transport was calculated as $ETR = Y_{(II)} \times PPFD \times 0.5$, where PPFD is the photosynthetic photon flux density. Also, quantum yields of non-light-induced nonphotochemical fluorescence quenching [$Y_{(NO)}$] and light-induced nonphotochemical fluorescence quenching regulated [$Y_{(NPQ)}$] were calculated using *Junior-PAM* software according to Kramer *et al.* (2004). Here, $Y_{(NO)} = 1/\{NPQ + 1 + [q_L \times (F_v/F_o)]\}$ and $Y_{(NPQ)} = 1 - Y_{(II)} - Y_{(NO)}$, where $q_L = (F_o'/F') \times [(F_m' - F')/(F_m' - F_o')]$.

O_2 gas exchange: The O_2 gas-exchange rate was measured using the oxygraphy + oxygen electrode system (*Hansatech Instruments*, UK) and *DW1/AD* chamber with integral Clark-type polarographic oxygen electrode (*Hansatech Instruments*, UK) at a light intensity of 1,200 μmol(photon) m^{-2} s^{-1} and a temperature of 28°C (Bil' *et al.* 1985, Biel *et al.* 2010). The chamber was loaded with 50 mg of thinly sliced leaf tissue in 2.5 ml of 50 mM potassium phosphate buffer (pH 7.5) taken immediately after opening the chamber. The O_2 evolution reaction was initiated by adding an excess amount of $NaHCO_3$ (10 mM, final concentration), sufficient to saturate photosynthesis with a carbon source, or the same amount of KNO_2 or KNO_3 as alternative electron acceptors. The measurements were carried out with constant stirring of the samples. Photosynthetic O_2 evolution was calculated taking into account dark respiration after 15-min incubation of the samples in the dark. The O_2 light curve fit parameters for the leaf gas exchange of wheat plants were calculated using the Prioul and Chartier (1977) model and the *Photosyn Assistant* software (Parsons and Ogston 1998).

H_2O_2 content: The H_2O_2 content in leaves was estimated according to Velikova *et al.* (2000). Fresh leaf mass (500 mg) was ground in 5 ml of 0.1% (w/v) trichloroacetic acid in an ice bath. The homogenate was centrifuged at 10,000 × *g* for 15 min. The supernatant of 0.5 ml was adjusted to 1 ml with 10 mM potassium phosphate buffer (pH 7.0), to which 1 ml of 1 M KI was added. Absorbance was measured on a *Genesis 10 UV* device (*Spectronic Unicam*, USA) at a wavelength of 390 nm.

Malondialdehyde content: The degree of lipid peroxidation was determined by measuring the content of malondialdehyde (MDA) according to Zhang *et al.* (2007). Fresh leaf tissue (0.5 g) was homogenized in 5 ml of 5% trichloroacetic acid and centrifuged at 5,000 × *g* for 20 min at 4°C. The supernatant of 1.5 ml was added to 2.5 ml of a reaction solution containing 20% TCA and 0.5% 2-thiobarbituric acid. The mixture was kept at 100°C for 25 min, after which it was cooled at room temperature and centrifuged at 5,000 × *g* for 10 min. Absorbance was measured on a *Genesis 10 UV* device (*Spectronic Unicam*, USA) at 532 nm. The value has been corrected for nonspecific absorbance at 600 nm. The concentration of MDA was calculated using an extinction coefficient of 155 μmol^{-1} cm^{-1} and expressed as μmol g^{-1}(FM).

Preparation of extracts and determination of nitrate reductase activity: Maximum nitrate reductase (NR, EC 1.6.6.1) capacity (NR_{max}) was determined by the method of Abd-El Baki *et al.* (2000). Leaf extracts were obtained 3 h after the onset of illumination when the NR activity reached its maximum value (Man *et al.* 1999). The fresh mass of leaves (0.4 g) was ground in a porcelain mortar with the addition of liquid nitrogen. Frozen samples were supplemented with 3 ml of isolation medium containing 100 mM HEPES–KOH, pH 7.6, 20 mM ethylenediaminetetraacetic acid (EDTA), 5 mM dithiothreitol (DTT), 10 μM flavin adenine dinucleotide phosphate (FADP), 10 μM leupeptin, 0.2 mM phenylmethylsulfonyl fluoride (PMSF), 1 mM Pefabloc, 0.6% polyvinylpolypyrrolidone, and 0.05% casein. The suspension was centrifuged at 16,000 × *g* for 12 min at 4°C. The supernatant was taken and stored at 4°C. The reaction mixture contained 50 mM HEPES–KOH (pH 7.6), 5 mM KNO_3, 0.2 mM NADH, 10 μM FADP, 1 mM DTT, and 20 mM EDTA in a final volume of 1.6 ml. The reaction was started by adding 0.4 ml of the plant extract. The incubation was carried out for 30 min at 30°C in the dark. The reaction was stopped by adding 0.1 ml of 500 mM zinc acetate solution. After centrifugation at 16,000 × *g* (5 min, 4°C), 0.1 ml of 0.3 mM phenazine methosulfate was added to the supernatant to oxidize excess NADH. The enzyme activity was judged by the amount of formed nitrite, which was determined by adding 1 ml of 1% sulfanilamide and 1 ml of 0.02% naphthyl ethylenediamine to the samples. After 5 min of color development, the samples were centrifuged for 5 min at 10,000 × *g*. The absorbance was determined on a *Genesis 10 UV* device (*Spectronic Unicam*, USA) at 546 nm against a solution containing all components of the incubation medium except for NADH. To construct the calibration curve, we used potassium nitrite solutions in an incubation medium without plant extract. The activity was expressed as μmol(NO_2) mg^{-1}(protein) h^{-1}.

Enzyme extracts for determining the activities of nitrite reductase, glutamine synthetase, and NAD-dependent glutamate dehydrogenase: Obtaining enzyme extracts for determining the activities of nitrite reductase (NiR, EC 1.6.6.4), glutamine synthetase (GS), and glutamate dehydrogenase (NAD-GDH) was carried out according to Robredo *et al.* (2011). Fresh leaf mass of 0.4 g was ground in a porcelain mortar with liquid nitrogen. Thereafter, 3 ml of a buffer solution containing 50 mM HEPES–KOH, pH 7.8, 5 mM DTT, 5 mM $MgCl_2$, 0.5 mM Na_2–EDTA, 0.5 mM PMSF, 20% glycerol, and 0.6% polyvinyl-polypyrrolidone were added. The suspension was centrifuged for 20 min at 4°C and 16,000 × *g*, and the supernatant was separated and stored at 4°C.

Nitrite reductase activity: The determination of NiR activity was carried out according to Fry *et al.* (1982). The reaction mixture contained 50 mM K-phosphate buffer (pH 7.0), 0.25 mM KNO_2, 0.5 mM methyl viologen (MV^{2+}), 2.5 mg Na dithionite, and 0.5 ml of plant extract in a final volume of 2.5 ml. After incubation for 10 min at 30°C, the reaction mixture was shaken vigorously until the blue color disappeared. The enzyme activity was determined by the rate of nitrite utilization, which was assessed by the difference in its concentration in the incubation medium without Na dithionite and the experimental sample. The nitrite concentration was determined as described for NR with absorption measurements at 540 nm. The activity was expressed as μmol(NO_2) mg^{-1}(protein) h^{-1}.

Glutamine synthetase activity: Glutamine synthetase **(**GS, EC 6.3.1.2) activity was determined according to Lacuesta *et al.* (1990). The reaction mixture contained 100 mM HEPES–KOH (pH 7.8), 150 mM Na–glutamate, 10 mM $MgCl_2$, 15 mM ATP, 10 mM $NH_2OH{\cdot}HC1$ (freshly prepared at pH 7.8), and 2 mM EDTA in a final volume of 3 ml. The reaction was started by adding 0.3 ml of the extract. After incubation for 30 min at 30°C, the reaction was stopped by adding 3 ml of a solution containing 8% (w/v) trichloroacetic acid, 3.3% (w/v) $FeCl_3$, and 2M HCl. After centrifugation at 5,000 × *g*, absorbance was measured at 540 nm. The calculations were performed taking into account the molar absorption coefficient of the γ-glutamyl hydroxamate–Fe^{3+} complex, equal to 0.85 × 10^3 M cm^{-1}. The activity was expressed as μmol(γ-GHM) mg^{-1}(protein) h^{-1}.

NAD-dependent glutamate dehydrogenase activity: NAD-dependent glutamate dehydrogenase (NAD-GDH, EC 1.4.1.2) activity was determined as described by Turano *et al.* (1996). The reaction mixture contained 100 mM Tris–HCl (pH 9.0), 0.25 mM NAD, 35 mM Na–glutamate, and 1 mM $CaCl_2$ in a final volume of 3 ml. After pre-incubation for 5 min at 30°C, the reaction was started by adding 0.2 ml of the enzyme extract and incubated for 10 min at 30°C. The reaction rate was judged by the amount of NADH formed by measuring the absorbance at 340 nm. A mixture without glutamate was used as a reference solution. The activity was expressed as μmol(NADH) mg^{-1}(protein) h^{-1}.

Proline dehydrogenase activity: Proline dehydrogenase (ProDH, EC 1.5.5.2) activity was determined according to Li *et al.* (2013). To extract the enzyme, 0.4 g of fresh leaves were homogenized in a porcelain mortar with liquid nitrogen and suspended in 3 ml of isolation medium containing 100 mM phosphate buffer (pH 8.0), 1 mM DTT, and 0.1 mM EDTA. After centrifugation at 12,000 × *g* for 10 min and 4°C, the supernatant was used to determine the enzyme activity. The reaction mixture containing 100 mM Na_2CO_3–$NaHCO_3$ buffer (pH 10.3), 10 mM NAD, and 20 mM L-proline was incubated for 10 min at 30°C. The enzyme activity was judged by the formation of NADH, the concentration of which was determined from the change in absorption at 340 nm. The activity was expressed as μmol(NADH) mg^{-1}(protein) h^{-1}.

Proline content: Determination of the amount of free proline (Pro) was carried out according to the method of Bates *et al.* (1973). Dry plant material (20 mg) was homogenized in 4 ml of 3% sulfosalicylic acid. After

centrifugation at 15,000 × *g* for 15 min, 2 ml of the supernatant was mixed with 2 ml of glacial acetic acid and 2 ml of ninhydrin solution (2.5% ninhydrin was dissolved in a mixture of glacial acetic acid and 6 M phosphoric acid, 3/2, v/v). The reaction mixture was incubated at 100°C for 1 h. The reaction was stopped by placing the samples in an ice bath, then 4 ml of toluene was added, shaken, and the absorbance of the toluene fraction was measured at 520 nm. Pro content [μg g^{-1}(DM)] was determined from a calibration curve.

Protein content was determined according to the method of Bradford (1976) using bovine serum albumin as a standard.

Statistical analysis: Recorded mean values are from three independent experiments with three repetitions in each. Statistical data processing was carried out using the *Statistica 10* software (*StatSoft Inc*., USA). The significance of differences between the mean values of the measured indicators was assessed using a one-way analysis of variance *ANOVA* (*Duncan*'s test). Calculations were performed at a given significance level $p \leq 0.05$. The differences between the two variants were analyzed by the *Student*'s *t*-test at the 5% significance level. The tables and figures show the mean values with standard errors from three–four biological replicates (n = 3–4).

Results

Growth processes: The intensity of growth processes was assessed by the determination of leaf dry mass (DM) in control plants from the beginning of seed germination (Fig. 1). It was shown that during 22 d the plants developed three leaves (Fig. 1). At the same time, some of the 10-d-old seedlings at the beginning of the growth of the second leaf were placed in a sealed chamber for incubation at a low CO_2 concentration, where it was impossible to determine the growth parameters. Therefore, the measurement of DM accumulation at low CO_2 was carried out only after opening the incubation chamber (Table 1). From a comparison of the data presented in Fig. 1 and Table 1, one can see that when the plants were placed in the chamber, the 1st leaf had already finished its growth and the low concentration of CO_2 did not affect the accumulation of its biomass, as evidenced by the absence of differences in the accumulation of DM of the leaves at any concentration of CO_2.

On the contrary, the development of the 2nd and 3rd leaves occurred during the period of being in the chamber at a low CO_2 concentration. Although the 2nd leaf appeared even before being placed in the chamber, the biomass accumulation of this leaf after incubation at low CO_2 concentration was 32% lower compared to the control. It should be noted that on the 20th day from seed germination, the growth of the second leaf stopped both in plants after incubation at low CO_2 and in control plants. The biomass of the 3rd leaf after incubation in a chamber at a low CO_2 concentration was 23% lower than that of control plants. Subsequently, all studies were carried out only on the 2nd leaf as the most sensitive to the effect of low CO_2 concentration.

O_2 gas exchange: After incubation of plants at low CO_2 concentration with the addition of $NaHCO_3$ as a source of CO_2 into the Clark cell as the electron acceptor for ETC, a lower rate of photosynthesis was observed compared to plants at natural CO_2 concentration (Fig. 2*A*). In contrast, when NO_2^- was used as an electron acceptor, the rate of photosynthesis was similar to control plants (Fig. 2*B*). In the case of using NO_3^-, the difference between the treatments was also insignificant (Fig. 2*C*).

In control plants, as a result of this, the value of P_N decreased in the order $CO_2 > NO_2^- > NO_3^-$. More precisely,

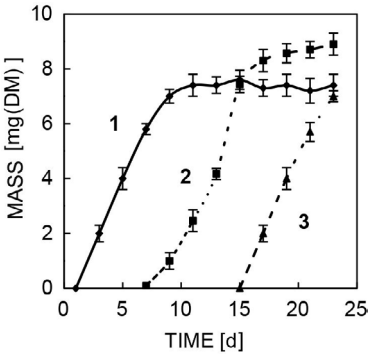

Fig. 1. Accumulation of dry mass (DM) in the 1st (1), 2nd (2), and 3rd (3) leaf of wheat seedlings at normal CO_2 concentration (Control). Data are means ± SE.

Table 1. Accumulation of dry biomass (DM [mg per leaf]) of leaves after incubation of wheat seedlings at a low concentration of carbon dioxide, after opening the chamber immediately (0 d) and for 2 d (–CO_2). For comparison, DM accumulation is shown in leaves of seedlings of similar age grown at normal CO_2 concentration (Control). Data are means ± SE. Values between columns 'Control' and '–CO_2' marked with *different letters* differ at the $p<0.05$ level, n = 4.

Days	1st leaf		2nd leaf		3rd leaf	
	Control	–CO_2	Control	–CO_2	Control	–CO_2
0	7.5 ± 0.3^a	7.4 ± 0.4^a	8.7 ± 0.3^a	5.9 ± 0.2^a	4.5 ± 0.3^b	3.5 ± 0.3^b
1	7.2 ± 0.4^a	7.5 ± 0.3^a	8.7 ± 0.3^a	5.8 ± 0.3^a	5.7 ± 0.3^b	4.5 ± 0.2^b
2	7.3 ± 0.4^a	7.4 ± 0.2^a	8.8 ± 0.4^a	6.0 ± 0.3^a	6.3 ± 0.4^{ab}	5.1 ± 0.2^{ab}

after incubating the plants at low CO_2 concentration, the rates of O_2 evolution were almost the same when using CO_2 treatment (Fig. 2*A*) and NO_2^- (Fig. 2*B*) as an electron acceptor, but significantly less when using NO_3^- (Fig. 2*C*).

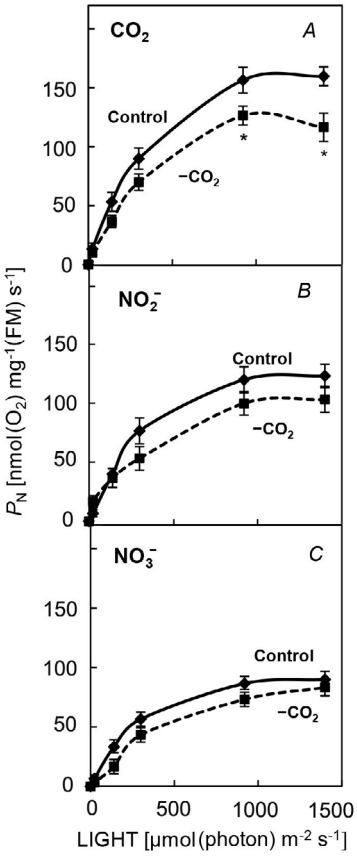

Fig. 2. Light curves of O_2 gas exchange in 2nd leaves after incubation of plants under conditions of normal (Control) and low ($–CO_2$) carbon dioxide concentration in the atmosphere using additions of $NaHCO_3$ (*A*), or KNO_2 as a source of NO_2^- (*B*) and KNO_3 as a source of NO_3^- (*C*). Data are means ± SE. Values between curves 'Control' and '$–CO_2$' marked with an asterisk differ at the $p<0.05$ level.

Analysis of the photosynthesis light curves (Table 2) using the model of Prioul and Chartier (1977) showed that after exposure of plants to a reduced CO_2 concentration, a decrease in the rate and quantum yield of photosynthesis was observed. The rate and quantum yield of photosynthesis were 68.2 and 62.8% of the level in control plants, respectively. A decrease in the rate of dark respiration, a decrease in the light-compensation point and in the light intensity, at which the light curve of photosynthesis saturates, was also found.

The use of KNO_2 led to a decrease in the rate of photosynthesis in comparison with the CO_2 treatment in the reaction medium. However, compared with control plants, we did not observe significant differences in the rate of gas exchange at the plateau of the light curve, quantum yield of photosynthesis, rate of dark respiration, light-compensation point, and light intensity at saturation of the photosynthesis light curve.

The introduction of KNO_3 as a source of NO_3^- into the reaction medium led to a significant decrease in the rate and quantum yield of photosynthesis, compared to leaves using additions of CO_2 and KNO_2 as a source of NO_2^- and control plants, but did not affect the gas exchange rate at the light curve plateau. However, in this case, an increase in the light-compensation point and light intensity for saturation of the photosynthesis light curve was observed.

Leaf fluorescence: After exposure of plants to low CO_2 concentration, there was a significant change in many fluorescence parameters of the second leaf in comparison with control plants (Fig. 3). Immediately after opening the chamber, low values of the maximal (F_v/F_m) and effective quantum [$Y_{(II)}$] yields, as well as the rate of noncyclic electron transport (ETR), were found. Subsequently, on the 2nd day after the opening of the chamber, values of $Y_{(II)}$ and ETR returned to control levels, and the value of F_v/F_m exceeded the control level at the natural concentration of CO_2. The values of the

Table 2. Parameters of light curves approximation of O_2 gas exchange according to the Prioul and Chartier model using different electron acceptors (CO_2 assimilation system, NO_2^-, and NO_3^-) in the 2nd leaf of wheat seedlings immediately after opening the incubation chamber of plants at low CO_2 concentration. For comparison, the parameters of plants of the same age grown at normal CO_2 concentration (Control) are shown. Data are means ± standard error. Values between columns 'Control' and '$–CO_2$' marked with *different letters* differ at the $p<0.05$ level, $n = 4$.

Electron acceptors	CO_2 assimilation system		NO_2^-		NO_3^-	
Variants	Control	$–CO_2$	Control	$–CO_2$	Control	$–CO_2$
Gas-exchange rate on the light curve plateau [nmol(O_2) mg^{-1}(FM) s^{-1}]	173 ± 8^{a}	118 ± 6^{bc}	137 ± 7^{b}	127 ± 7^{b}	99 ± 5^{c}	94 ± 5^{c}
O_2-evolution rate in the dark [nmol(O_2) mg^{-1}(FM) s^{-1}]	96.3 ± 6.2^{a}	37.2 ± 1.9^{d}	51.8 ± 2.5^{c}	56.3 ± 3.1^{bc}	66.7 ± 3.3^{b}	51.1 ± 2.5^{c}
Quantum yield of photosynthesis	0.36 ± 0.02^{a}	0.23 ± 0.01^{c}	0.28 ± 0.01^{b}	0.29 ± 0.01^{b}	0.28 ± 0.02^{ab}	0.16 ± 0.08^{d}
Light-compensation point [µmol(photon) m^{-2}s^{-1}]	266 ± 15^{ab}	163 ± 9^{c}	182 ± 10^{c}	196 ± 10^{c}	243 ± 12^{b}	312 ± 16^{a}
The light intensity when the light curve is saturated [µmol(photon) m^{-2}s^{-1}]	743 ± 37^{ab}	681 ± 34^{b}	656 ± 33^{b}	638 ± 32^{b}	604 ± 30^{b}	888 ± 44^{a}

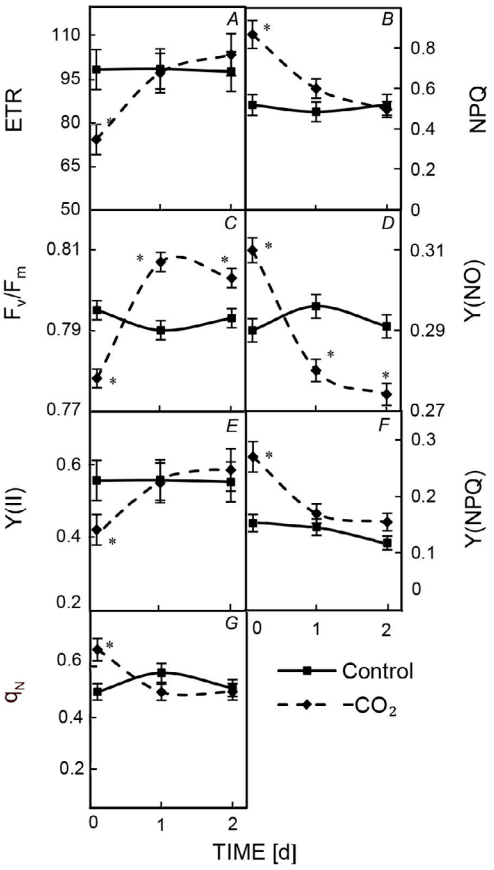

Fig. 3. Fluorescence parameters of 2nd leaf immediately after opening the incubation chamber with plants at a low concentration of CO_2 and during the next 2 d ($–CO_2$) in comparison with plants growing at a natural concentration of CO_2 (Control). Data are means ± SE. Values between curves 'Control' and '$–CO_2$' marked with an asterisk differ at the $p<0.05$ level. Here, ETR – electron transport rate, F_v/F_m and $Y_{(II)}$ – PSII maximal and effective quantum yields, respectively, q_N and NPQ – parameters of nonphotochemical quenching. $Y_{(NO)}$ – non-light-induced nonphotochemical fluorescence quenching and $Y_{(NPQ)}$ – light-induced nonphotochemical fluorescence quenching regulated.

coefficient of photochemical quenching of fluorescence (q_P) showed insignificant changes both after exposure to a low concentration of CO_2 and after returning to the natural concentration of CO_2. The values of NPQ and q_N after increasing at low CO_2 then returned to initial levels at the natural concentration of CO_2. The values of the $Y_{(NPQ)}$, which determine light-induced nonphotochemical quenching of fluorescence, and $Y_{(NO)}$, which are associated with non-light-induced quenching of fluorescence, significantly exceeded the levels of control plants indicated immediately after opening the chamber. Subsequently, after exposure to the natural concentration of CO_2, the $Y_{(NPQ)}$ values decreased to the control level, whereas the $Y_{(NO)}$ values fell below the corresponding values in the control plants.

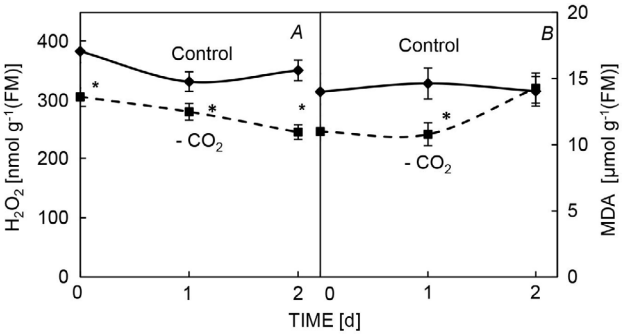

Fig. 4. The content of H_2O_2 (*A*) and malondialdehyde (MDA) (*B*) in the 2nd leaves immediately after opening the incubation chamber at low CO_2 concentration and during the next 2 d ($–CO_2$) in comparison with plants growing at a natural CO_2 concentration (Control). Data are means ± SE. Values between curves 'Control' and '$–CO_2$' marked with an asterisk differ at the $p<0.05$ level.

Assessment of oxidative stress: The degree of development of oxidative stress was judged by the content of malondialdehyde (MDA) and H_2O_2. Immediately after opening the chamber for exposing plants to low CO_2 concentration, the H_2O_2 content in the leaves was lower than that in the control plants, and this tendency was maintained for 2 d of plant exposure to natural CO_2 concentration (Fig. 4*A*). Similar data were obtained for the MDA content; however, in this case, the MDA contents in the leaves of plants exposed to low CO_2 concentration, after 2 d of exposure to natural CO_2 concentration, was comparable to the level in control plants (Fig. 4*B*).

The activity of nitrogen-metabolism enzymes: After incubation of plants at a reduced CO_2 concentration, a significant change in the activity of enzymes of nitrogen metabolism was observed. Immediately after opening the chamber, lowered NR activity was indicated in the leaves compared to control plants (Fig. 5*A*). The low level of NR activity was also observed for the next 2 d already at the natural CO_2 concentration.

The NiR activity after incubation of plants at a reduced CO_2 concentration was slightly higher than that in control plants (Fig. 5*B*). Subsequently, the activity of the enzyme increased on the first day and decreased almost to the control level on the second day in an atmosphere of the natural CO_2 concentration. The GS activity strongly increased at the CO_2 deficiency in comparison with the control plants, but on the second day after the opening of the chamber, it gradually decreased to the control level at natural CO_2 concentration (Fig. 5*C*).

The NAD-GDH activity in leaves remained unchanged after incubation of plants at a reduced CO_2 concentration, but increased sharply the next day after opening the chamber (Fig. 5*D*). Then, the NAD-GDH activity decreased slightly, but continued to remain at a level significantly higher than the values in control plants.

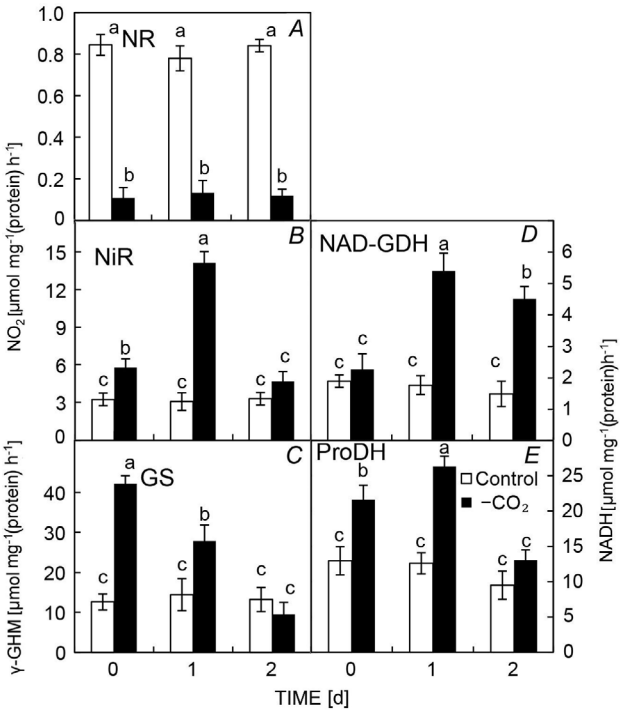

Fig. 5. Activity of nitrogen metabolism enzymes in 2nd leaf during natural CO_2 concentration (0, Control) and after incubation at a low concentration of CO_2 ($–CO_2$), immediately after opening the chamber (0 d) and during the next 2 d. (*A*) Nitrate reductase activity (NR); (*B*) nitrite reductase (NiR); (*C*) glutamine synthetase (GS); (*D*) glutamate dehydrogenase (NAD-GDH); (*E*) proline dehydrogenase (ProDH). Data are means ± SE. Values between columns 'Control' and '$–CO_2$' marked with an asterisk differ at the $p<0.05$ level.

ProDH activity at low CO_2 concentration was twofold higher than the activity of control plants immediately after opening the incubation chamber and remained high during the next day (Fig. 5*E*). However, on the second day, under natural CO_2 concentration, the ProDH activity significantly decreased and became comparable to the values in control plants.

Proline content: The content of free Pro in leaves after incubation of plants at the natural CO_2 concentration increased 2 times as compared to leaves in the control (Fig. 6). However, after a while the Pro content decreased achieving the control level.

Discussion

By the beginning of the experiment with the exposure of plants at a reduced concentration of CO_2 in all groups of plants, the first leaf had already completed its growth and subsequently did not react to changes in the concentration of carbon dioxide in the air. In this case, the first leaf was already an aging organ, in which catabolic processes were intensified, accompanied by the breakdown of proteins and the accumulation of nitrogen-containing compounds.

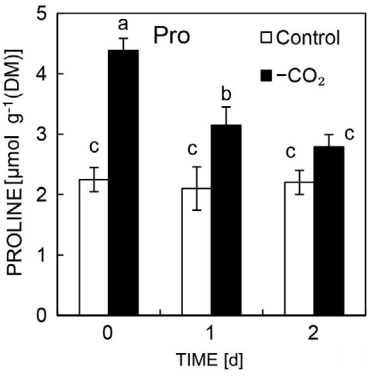

Fig. 6. Proline content in 2nd leaf during natural CO_2 concentration (Control) and after incubation at a low concentration of CO_2 ($–CO_2$), immediately after opening the chamber (0 d) and during the next 2 d. Data are means ± SE. Data are means ± SE. Values between columns 'Control' and '$–CO_2$' marked with an asterisk differ at the $p<0.05$ level.

In addition, the outflow of substances from old leaves to sink organs usually takes place (Masclaux-Daubresse *et al.* 2002, Sharma *et al.* 2011). In our experiment, the 3rd leaf can act as a sink organ. Thus, one can explain why the growth of the third leaf was a little dependent on the carbon deficit. On the contrary, the second leaf was in a stage of active growth, which requires large amounts of carbon dioxide. This leaf had a pronounced growth arrest response with a decrease in CO_2 concentration (Table 1). That is why the 2nd leaf was chosen for further research.

We showed that low CO_2 concentration decreased the rate and quantum yield of photosynthesis when $NaHCO_3$ was added for activation of the process of CO_2 fixation. Analysis of the fluorescence parameters (Fig. 3) showed that the exposure of plants to a low concentration of CO_2 in the atmosphere decreased the maximum (F_v/F_m) and effective [$Y_{(II)}$] PSII quantum yields, as well as the photochemical quenching of fluorescence (q_P and q_L, reflecting the fraction of open reaction centers). This means that CO_2 deficiency reduces not only the rate of photosynthesis but also primary photochemical processes.

The return of plants to conditions of natural CO_2 concentration after opening the chamber led to an increase in the maximum quantum yield to values higher than the level in control plants. The dynamics of changes in the value of the effective quantum yield $Y_{(II)}$ had a similar character, but its values were at the control level already the next day after the opening of the chamber and did not change subsequently. The rate of electron transport through PSII (ETR) in the process of plant adaptation changed similarly to $Y_{(II)}$. The value of nonphotochemical quenching of the fluorescence of chlorophyll *a* PSII (NPQ), which characterizes the level of thermal dissipation of the absorbed energy of the light flux, significantly decreased during the first day at a natural concentration of CO_2 and reached the control level on the second day. In this case, an increase in the coefficient of nonphotochemical quenching of fluorescence (q_N) was observed.

Thus, under conditions of low CO_2 concentration, a decrease in the activity of some reactions of the light stage of photosynthesis, limiting the rate of photosynthesis, was observed.

The energy absorbed by chlorophyll can be partially dissipated in the form of heat (nonphotochemical quenching of fluorescence) (Qiu *et al.* 2003), but can also be used to reduce NO_2^-, which can act as an alternative electron acceptor (Eichelmann *et al.* 2011). On the one hand, this makes it possible to utilize the excess energy of absorbed sunlight. On the other hand, by changing the ratio of the flow of electrons from the ETR to various acceptors, one can regulate the C/N exchange, *i.e.*, change the ratio of carbohydrate and nitrogen-containing metabolites. Indeed, the incubation of plants at a low CO_2 concentration had little effect on the rate of light-dependent O_2 evolution when using NO_2^- as the electron acceptor in comparison with control plants (Fig. 2). At the same time, no significant differences from control plants were observed in the rate of gas exchange at the plateau of the light curve, the quantum efficiency of photosynthesis, the rate of dark respiration, the light-compensation point, and the intensity of light at saturation of the light curve of photosynthesis (Table 2). Consequently, with a slowdown in the processes of carbon metabolism, the pathway of the utilization of electrons from the photosynthetic electron transport chain, aimed at the primary assimilation of nitrogen, continued to function successfully.

Our results are in agreement with the data of Zivcak *et al.* (2013) on the action of moderate dehydration on wheat plants. Drought led to stomatal closure in wheat associated with a very low intercellular CO_2 concentration. The results obtained in the study suggest an important role of alternative electron sinks (either from PSII or PSI) and cyclic electron flow in the photoprotection of PSII and PSI under drought-stress conditions.

After incubation of plants at low CO_2 concentration, a decrease in the rate of O_2 evolution was observed when using CO_2 as an addition, which turned out to be comparable to that when using NO_2^- as an acceptor (Fig. 2). Consequently, the exposure of plants to a low CO_2 concentration led to a change in the ratio of the direction of the ETC electron flux, namely, a decrease in the CO_2 reduction rate and a relative increase in the NO_2^- reduction rate. The addition of NO_3^- to the reaction mixture was also accompanied by the evolution of O_2, although it is believed that the NO_3^- reduction reaction is not light-dependent. This process, most likely, can occur indirectly and includes the intermediate enzymatic conversion of NO_3^- to NO_2^-.

At a natural concentration of CO_2, the main flow of absorbed solar energy is directed to the reduction of carbon compounds, even though it is divided approximately equally between C and N reduction. Under natural conditions, the predominance of CO_2 reduction is explained by the fact that 8 e^- is required for the photoassimilation of each NO_2^- molecule in Glu, compared to 4 e^- for CO_2 assimilation (Robinson 1986). However, the enzymatic capacity of NO_2^- photoreduction in the presence of available substrates can be comparable to CO_2 reduction (Eichelmann *et al.* 2011). In the course of our experiment, we also observed that at the natural concentration of CO_2, the efficiency of using various electron acceptors in the ETC of photosynthesis decreases in the series of substances added to leaf segments as a course of CO_2, NO_2^-, and NO_3: $CO_2 > NO_2^- > NO_3^-$ (Fig. 2). It is also important to note that at a saturating concentration of CO_2, the rate of carbon dioxide fixation increases with the simultaneous presence of NO_2^- photoreduction. Apparently, in this case, the reduction of NO_2^- contributes to the maintenance of the balance of ATP and NADPH (Robinson 1986).

After exposing plants to an atmosphere with a low concentration of carbon dioxide, all the main parameters of photosynthesis decreased when bicarbonate was added to the reaction medium (Fig. 2, Table 2). However, they remained unchanged when using NO_2^- as an acceptor. Consequently, when the processes of carbon metabolism slow down, the pathway of primary assimilation of nitrogen continues to function successfully. This is also confirmed by the data of measurements of the enzymatic activity of NiR (Fig. 5*B*), the reaction rate of which changed little after incubation of plants at a low CO_2 concentration. An increase in enzyme activity on the second day after the opening of the chamber may be associated with an intensification of carbon metabolism under conditions of natural CO_2 concentration (Plaut *et al.* 1977). On the 2nd day after the opening of the chamber, the activity of the enzyme returned to its initial level, most likely due to the work of the mechanisms that maintain the constant C/N balance.

The use of light energy to reduce NO_2^- occurs in an Fd-dependent NiR reaction with the formation of NH_3. In this reaction, reduced Fd integrated into the electron transport chain of PSI is used as a redox factor. Since the reduction of both NO_2^- and CO_2 compete for the same pool of reducing agents with similar properties (Eichelmann *et al.* 2011), the Fd site forms a nodal point in the regulation of nitrogen and carbon metabolism, influencing the distribution of electrons in the chloroplast ETC between different metabolic processes (Hanke *et al.* 2011).

The phenomenon of O_2 release upon the addition of NO_3^- to the reaction medium of the Clarke cell is rather difficult to explain since it is believed that nitrate reduction in higher plants is not a light-dependent process. Fd-dependent NR was found only in prokaryotic organisms and blue-green algae. However, in higher plants, NR is not Fd-dependent (Knaff and Hirasawa 1991), although it is a light-inducible enzyme (Jonassen *et al.* 2009). The most probable assumption seems to be that NO_3^- is preliminarily converted into NO_2^- in the cytoplasm with the help of NR, transported to chloroplasts, and only then participates in the light-dependent reaction with the help of NiR. However, this explanation has some contradictions. First of all, this is the difference in the rates of enzymatic reactions, which in NR is an order of magnitude lower than that of NiR, which is significantly lower than the observed rate of NO_3^- utilization as

compared to NO_2^- (Fig. 2, Table 2). Moreover, we have shown very low NR activity after incubation of plants at low CO_2 concentration. This issue requires additional research.

A change in the ratio of closely interrelated fluxes of carbon and nitrogen metabolism compounds leads to a disruption of the C/N balance, the invariability of which is maintained by numerous regulatory mechanisms. A decrease in the flow of carbon compounds can lead to a change in the activity of the main enzymes of nitrogen metabolism and an increase in the number of nitrogen compounds in the cell. Indeed, in our experiment, the growth of the second leaf of wheat seedlings under conditions of CO_2 deficiency was accompanied by a change in the activity of the main enzymes of nitrogen metabolism (Fig. 5). After incubation of the plants at a low CO_2 concentration, close to the CO_2-compensation point, a decrease in NR activity in the leaves was observed (Fig. 5*A*). It has previously been shown that illuminating leaves in a CO_2-free atmosphere results in inhibition of NR activity, which again increases with the addition of CO_2 (Kaiser and Förster 1989). The time for a 50% change in enzyme activity was 30 min. This implies the presence of a mechanism for rapid inactivation/activation of NR in leaves and a close relationship of the enzyme with photosynthetic processes. According to our data, after long-term incubation of plants under conditions of CO_2 deficiency, the restoration of NR activity to the initial level takes more than 2 d from the moment the chamber is opened, which is possibly associated with regulation at the level of gene expression. For example, it has been shown that the expression of NR genes can be regulated by light and sugars (Crawford 1995, Jonassen *et al.* 2009). On the other hand, the activity of the enzyme can decrease under the influence of reactive oxygen species (ROS) or as a result of the work of specific proteases, as well as under the combined action of these two factors that enhance the action of each other (Kenis *et al.* 1994). In our work, after incubation of plants under conditions of CO_2 deficiency, there was no increase in the accumulation of ROS; their concentration turned out to be even lower than that in control plants (Fig. 4). Considering the long recovery period of the enzyme activity, inhibition of the enzyme expression under conditions of carbohydrate deficiency, which is observed with CO_2 deficiency, is most likely.

After incubation of wheat seedlings under conditions of CO_2 deficiency, among other main enzymes of nitrogen metabolism, a significant increase in GS activity was observed, which subsequently gradually decreased to the control level in an atmosphere with natural CO_2 concentration (Fig. 5*C*). GS activity depends on environmental conditions and the metabolic status of plant tissues, including those that change during one day (Stitt *et al.* 2002). That is why our results may indicate a regulatory equalization of the imbalance in the activity of nitrogen metabolism enzymes caused by CO_2 deficiency. GS is central to the primary nitrogen assimilation pathway and the reassimilation of NH_4^+ produced by photorespiration (Miflin and Habash 2002). At normal CO_2 concentration in the environment, ribulose-1,5-bisphosphate carboxylase/oxygenase catalyzes two reactions in which CO_2 and O_2 compete for one active site of the enzyme to form 3-phosphoglycerate and phosphoglycerate, respectively (Lorimer 1981). With a CO_2 deficiency, the value of the oxygenase function of the enzyme increases, *i.e.*, the process of photorespiration is enhanced, as a result of which an excessive amount of ammonia is formed at a rate that is an order of magnitude higher than the reduction of NO_3^- in illuminated leaves. To maintain the nitrogen balance of the leaf, it is necessary to reassimilate the photorespiratory NH_3, otherwise, its concentration may increase to toxic levels (Osmond 1981). The photorespiratory NH_3 formed in mitochondria can be assimilated in chloroplasts using the GS/GOGAT system, but not GDH (Osmond 1981, Wallsgrove *et al.* 1983). At the same time, the consumption of additional energy required for NH_3-recirculation in photorespiration has relatively little effect on the ATP/NADPH stoichiometry and the electron transport chain speed (Osmond 1981). Since chloroplast GS is the main site of photorespiratory NH_3 reassimilation (Wallsgrove *et al.* 1983), an increase in the activity of this enzyme in the presence of CO_2 deficiency under the conditions of our experiment seems to be quite justified (Fig. 5*C*).

After incubation of plants under conditions of CO_2 deficiency, no changes in NAD-GDH activity were observed in our experiments (Fig. 5*D*) and, therefore, there was no increase in glutamate deamination, which may be due to the absence of ROS accumulation (Fig. 4). In this case, an increase in the concentration of glutamate in chloroplasts can occur not only as a result of an increase in the activity of the GS/GOGAT complex, but also of the transport of cytoplasmic glutamate, which is a product of the Pro/Δ^1-pyrroline-5-carboxylate cycle (Ben Rejeb *et al.* 2014). Glutamate is the main substrate for Pro synthesis. Increased utilization of glutamate may have contributed to the accumulation of Pro, which we observed after incubation of plants at low CO_2 (Fig. 6). On the contrary, under conditions of normal CO_2 concentration, after opening the chamber, the NAD-GDH activity significantly increased, which could lead to a decrease in the glutamate pool. This process coincided with the observed drop in the concentration of Pro in the leaves within several days after opening the incubation chamber (Fig. 6).

Free Pro accumulates in plants in response to a wide range of abiotic and biotic stresses. Most of the data on the regulation of Pro-metabolism were obtained on plants grown under conditions of salt and osmotic stress (Ivanov 2015). In our experiments with CO_2 deficiency, an increase in the Pro concentration in the leaves was also observed (Fig. 6). It should be noted that the value of Pro accumulation did not depend on the time of incubation of plants at reduced CO_2 (7, 10, or 14 d, data not shown). Therefore, in this case, we should not speak about the accumulation of Pro, but about the maintenance of its pool, when the synthesis is compensated by decay. This statement is supported by the observed increase in ProDH activity (Fig. 5*E*).

Pro synthesis can be considered as the process of final utilization of the energy of electrons coming from the photosynthetic electron transport chain. Therefore, there may be a decrease in the use of O_2 instead of NAD(P) as an electron acceptor in photosynthesis, which leads to a decrease in the accumulation of ROS and provides some protection against photoinhibition under unfavorable environmental conditions (Hare *et al.* 1998). Pro metabolism is directly related to NAD(P)H/NAD(P) redox balance, and Pro itself can act as a redox transporter (Sharma *et al.* 2011, Ben Rejeb *et al.* 2014, Giberti *et al.* 2014). Thus, the enhancement of Pro synthesis under stress may be part of the mechanism that maintains the redox potential of the cell at a level acceptable for metabolic processes (Hare *et al.* 1998).

Stomatal closure during osmotic stress limits carbon uptake, which subsequently leads to decreased NADPH consumption in the Calvin cycle. The use of NAD(P)H to synthesize Pro during stress may increase the NAD(P)/NAD(P)H ratio in the cell. It has been shown that under stress conditions Pro can be synthesized from Glu in chloroplasts (Székely *et al.* 2008). Therefore, regulation of the NAD(P)/NAD(P)H ratio can form a link between Pro biosynthesis and NAD(P) reduction involving two oxidative pentose phosphate pathway (OPPP) dehydrogenases that control the conversion of glucose-6-phosphate to ribulose-5-phosphate (Shetty 2004). In this case, the generation of CO_2 formed during the synthesis of ribulose-5-phosphate allows the process of carbon reduction under conditions of exogenous CO_2 deficiency to continue, and NAD(P)H can be used in Pro biosynthesis, which prevents photoinhibition and the production of excess ROS in the chloroplast (Sharma *et al.* 2011, Ben Rejeb *et al.* 2014).

On the other hand, in nonphotosynthetic plastids, the oxidation of glucose-6-phosphate *via* OPPP provides electrons for NiR and Fd-GOGAT (Oji *et al.* 1985, Bowsher *et al.* 1989, 1992). In this case, Fd:$NADP^+$-oxidoreductase (FNR, EC 1.18.1.2) mediates Fd reduction by NADPH provided by OPPP. Thus, Fd and FNR play a central role in the distribution of redox equivalents in both types of plastids (Sakakibara 2003). Since FNR carries out electron transfer from NADPH to nonphotosynthetic type Fd, the redox equivalent can be used *via* OPPP to reduce NO_3^- and in photosynthetic organs (Sakakibara 2003).

Conclusion: Thus, carbon and nitrogen metabolism are closely interrelated. Under conditions of CO_2 deficiency in the atmosphere, an increase in nitrogen metabolism in plant leaves is possible. To prevent C/N imbalance in cells, NR activity is inhibited first of all, which leads to a decrease in the amount of substrate for the light-dependent metabolism of NO_2^-. Utilization of already absorbed nitrite occurs along the pathway of Pro synthesis from Glu, which in this case acts as a by-product that utilizes the excess energy of absorbed photons during photosynthesis, and it can also be considered a metabolically neutral compound for storing excess nitrogen. That is, the formation of Pro under stress is not purposeful, but serves as a means of detoxifying cells from excess nitrogen. In stress-free conditions, the Pro pool is supported by a balanced synthesis and decay system. Under stressful conditions, when the only enzyme of Pro degradation, ProDH, is inhibited (Kiyosue *et al.* 1996), the cycle breaks and Pro accumulates. At the same time, the purpose and functions of this amino acid also change. These functions depend on the spatial and temporal regulation of Pro synthesis and catabolism, binding or releasing reductant and energy at the right place and time to meet the plant's needs, which is not consistent with the more-is-better theory in the case of Pro accumulation (Sharma *et al.* 2011). It is also possible that the purpose of the accumulation of Pro is not to counteract stress, but serves to restore the plant after the termination of stress.

References

Abd-El Baki G.K., Siefritz F., Man H.-M. *et al.*: Nitrate reductase in *Zea mays* L. under salinity. – Plant Cell Environ. **23**: 515-521, 2000.

Bates L.S., Waldren R.P., Teare I.D.: Rapid determination of free proline for water stress studies. – Plant Soil **39**: 205-207, 1973.

Ben Rejeb K., Abdelly C., Savouré A.: How reactive oxygen species and proline face stress together. – Plant Physiol. Bioch. **80**: 278-284, 2014.

Biel K.Y., Fomina I.R., Nazarova G.N. *et al.*: Untangling metabolic and spatial interactions of stress tolerance in plants. 1. Patterns of carbon metabolism within leaves. – Protoplasma **245**: 49-73, 2010.

Bil' K.Y., Fomina I.R., Tsenova E.N.: Effects of nitrogen nutrition on photosynthetic enzyme activities, type of photosynthates and photosystem 2 activity in maize leaves. – Photosynthetica **19**: 216-220, 1985.

Bowsher C.G., Boulton E.L., Rose J. *et al.*: Reductant for glutamate synthase is generated by the oxidative pentose phosphate pathway in non-photosynthetic root plastids. – Plant J. **2**: 893-898, 1992.

Bowsher C.G., Hucklesby D.P., Emes M.J.: Nitrite reduction and carbohydrate metabolism in plastids purified from roots of *Pisum sativum* L. – Planta **177**: 359-366, 1989.

Bradford M.M.: A rapid and sensitive method for the quantitation of microgram quantities of protein utilizing the principle of protein-dye binding. – Anal. Biochem. **72**: 248-254, 1976.

Coic Y., Lesaint C.: Comment assurer une bonne nutrition en eau et ions mineraux en horticulture? [How to ensure good water and mineral ion nutrition in horticulture?] – Horticulture Francaise **8**: 11-14, 1971. [In French]

Commichau F.M., Forchhammer K., Stülke J.: Regulatory links between carbon and nitrogen metabolism. – Curr. Opin. Microbiol. **9**: 167-172, 2006.

Crawford N.M.: Nitrate: nutrient and signal for plant growth. – Plant Cell **7**: 859-868, 1995.

Eichelmann H., Oja V., Peterson R.B., Laisk A.: The rate of nitrite reduction in leaves as indicated by O_2 and CO_2 exchange during photosynthesis. – J. Exp. Bot. **62**: 2205-2215, 2011.

Ferrario-Méry S., Valadier M.H., Godfroy N. *et al.*: Diurnal changes in ammonia assimilation in transformed tobacco plants expressing ferredoxin-dependent glutamate synthase mRNA in the antisense orientation. – Plant Sci. **163**: 59-67, 2002.

Fry I.V., Cammack R., Hucklesby D.P., Hewitt E.J.: Kinetics of leaf nitrite reductase with Methyl Viologen and ferredoxin

under controlled redox conditions. – Biochem. J. **205**: 235-238, 1982.

Giberti S., Funck D., Forlani G.: Δ^1-pyrroline-5-carboxylate reductase from *Arabidopsis thaliana*: stimulation or inhibition by chloride ions and feedback regulation by proline depend on whether NADPH or NADH acts as co-substrate. – New Phytol. **202**: 911-919, 2014.

Goltsev V.N., Kalaji H.M., Paunov M. *et al*.: Variable chlorophyll fluorescence and its use for assessing physiological condition of plant photosynthetic apparatus. – Russ. J. Plant Physiol. **63**: 869-893, 2016.

Hanke G.T., Satomi Y., Shinmura K. *et al*.: A screen for potential ferredoxin electron transfer partners uncovers new, redox dependent interactions. – BBA-Proteins Proteom. **1814**: 366-374, 2011.

Hare P.D., Cress W.A., Van Staden J.: Dissecting the roles of osmolyte accumulation during stress. – Plant Cell Environ. **21**: 535-553, 1998.

Ireland R.J., Lea P.J.: The enzymes of glutamine, glutamate, asparagine and aspartate metabolism. – In: Singh B.K. (ed.): Plant Amino Acids: Biochemistry and Biotechnology. Pp. 49-109. Marcel Dekker, New York 1999.

Ivanov A.A.: Response of wheat seedlings to combined effect of drought and salinity. – In: Tripathi B.N., Müller M. (ed.): Stress Responses in Plants. Mechanisms of Toxicity and Tolerance. Pp. 159-198. Springer, Cham 2015.

Jonassen E.M., Sandsmark B.A.A., Lillo C.: Unique status of NIA2 in nitrate assimilation: NIA2 expression is promoted by HY5/HYH and inhibited by PIF4. – Plant Signal. Behav. **4**: 1084-1086, 2009.

Kaiser W.M., Förster J.: Low CO_2 prevents nitrate reduction in leaves. – Plant Physiol. **91**: 970-974, 1989.

Kendall A.C., Wallsgrove R.M., Hall N.P. *et al*.: Carbon and nitrogen metabolism in barley (*Hordeum vulgare* L.) mutants lacking ferredoxin-dependent glutamate synthase. – Planta **168**: 316-323, 1986.

Kenis J.D., Rouby M.B., Edelman M.O., Silvente S.T.: Inhibition of nitrate reductase by water stress and oxygen in detached oat leaves: A possible mechanism of action. – J. Plant Physiol. **144**: 735-739, 1994.

Kiyosue T., Yoshiba Y., Yamaguchi-Shinozaki K., Shinozaki K.: A nuclear gene encoding mitochondrial proline dehydrogenase, an enzyme involved in proline metabolism, is upregulated by proline but downregulated by dehydration in *Arabidopsis*. – Plant Cell **8**: 1323-1335, 1996.

Knaff D.B., Hirasawa M.: Ferredoxin-dependent chloroplast enzymes. – BBA-Bioenergetics **1056**: 93-125, 1991.

Kramer D.M., Johnson G., Kiirats O., Edwards G.E.: New flux parameters for the determination of Q_A redox state and excitation fluxes. – Photosynth. Res. **79**: 209-218, 2004.

Lacuesta M., González-Moro B., González-Murua C., Muñoz-Rueda A.: Temporal study of the effect of phosphinothricin on the activity of glutamine synthetase, glutamate dehydrogenase and nitrate reductase in *Medicago sativa* L. – J. Plant Physiol. **136**: 410-414, 1990.

Lam H.-M., Coschigano K.T., Oliveira I.C. *et al*.: The molecular genetics of nitrogen assimilation into amino acids in higher plants. – Annu. Rev. Plant Phys. **47**: 569-593, 1996.

Li X., Yang Y., Jia L. *et al*.: Zinc-induced oxidative damage, antioxidant enzyme response and proline metabolism in roots and leaves of wheat plants. – Ecotox. Environ. Safe. **89**: 150-157, 2013.

Lorimer G.H.: The carboxylation and oxygenation of ribulose 1,5-bisphosphate. The primary events in photosynthesis and photorespiration. – Ann. Rev. Plant Physio. **32**: 349-383, 1981.

Man H.M., Abd-El Baki G.K., Stegmann P. *et al*.: The activation state of nitrate reductase is not always correlated with total nitrate reductase activity in leaves. – Planta **209**: 462-468, 1999.

Masclaux-Daubresse C., Valadier M.H., Carrayol E. *et al*.: Diurnal changes in the expression of glutamate dehydrogenase and nitrate reductase are involved in the C/N balance of tobacco source leaves. – Plant Cell Environ. **25**: 1451-1462, 2002.

Miflin B.J., Habash D.Z.: The role of glutamine synthetase and glutamate dehydrogenase in nitrogen assimilation and possibilities for improvement in the nitrogen utilization of crops. – J. Exp. Bot. **53**: 979-987, 2002.

Noctor G., Foyer C.H.: A re-evaluation of the ATP:NADPH budget during C_3 photosynthesis: a contribution from nitrate assimilation and its associated respiratory activity? – J. Exp. Bot. **49**: 1895-1908, 1998.

Oji Y., Watanabe M., Wakiuchi N., Okamoto S.: Nitrite reduction in barley root plastids: dependence on NADPH coupled with glucose-6-phosphate and 6-phosphogluconate dehydrogenase, and possible involvement of an electron carrier and a diaphorase. – Planta **165**: 85-90, 1985.

Osmond C.B.: Photorespiration and photoinhibition. Some implications for the energetics of photosynthesis. – BBA-Rev. Bioenergetics **639**: 77-98, 1981.

Parsons R., Ogstone S.A.: Photosyn assistant Windows software for analysis of photosynthesis. Dundee Scientific, Scotland 1998.

Plaut Z., Lendzian K., Bassham J.A.: Nitrite reduction in reconstituted and whole spinach chloroplasts during carbon dioxide reduction. – Plant Physiol. **59**: 184-188, 1977.

Prioul J.L., Chartier P.: Partitioning of transfer and carboxylation components of intracellular resistance to photosynthetic CO_2 fixation: A critical analysis of the methods used. – Ann. Bot.-London **41**: 789-800, 1977.

Qiu N., Lu Q., Lu C.: Photosynthesis, photosystem II efficiency and the xanthophyll cycle in the salt-adapted halophyte *Atriplex centralasiatica*. – New Phytol. **159**: 479-486, 2003.

Robinson J.M.: Carbon dioxide and nitrite photoassimilatory processes do not intercompete for reducing equivalents in spinach and soybean leaf chloroplasts. – Plant Physiol. **80**: 676-684, 1986.

Robredo A., Pérez-López U., Miranda-Apodaca J. *et al*.: Elevated CO_2 reduces the drought effect on nitrogen metabolism in barley plants during drought and subsequent recovery. – Environ. Exp. Bot. **71**: 399-408, 2011.

Sakakibara H.: Differential response of genes for ferredoxin and ferredoxin:$NADP^+$ oxidoreductase to nitrate and light in maize leaves. – J. Plant Physiol. 160: 65-70, 2003.

Sánchez-Rodríguez E., Rubio-Wilhelmi M.M., Rios J.J. *et al*.: Ammonia production and assimilation: its importance as a tolerance mechanism during moderate water deficit in tomato plants. – J. Plant Physiol. **168**: 816-823, 2011.

Sharma S., Villamor J.G., Verslues P.E.: Essential role of tissue-specific proline synthesis and catabolism in growth and redox balance at low water potential. – Plant Physiol. **157**: 292-304, 2011.

Shetty K.: Role of proline-linked pentose phosphate pathway in biosynthesis of plant phenolics for functional food and environmental applications: a review. – Process Biochem. **39**: 789-803, 2004.

Stitt M., Müller C., Matt P. *et al*.: Steps towards an integrated view of nitrogen metabolism. – J. Exp. Bot. **53**: 959-970, 2002.

Székely G., Ábrahám E., Cséplő A. *et al*.: Duplicated *P5CS* genes of *Arabidopsis* play distinct roles in stress regulation and developmental control of proline biosynthesis. – Plant J.

53: 11-28, 2008.
Terashima I., Yanagisawa S., Sakakibara H.: Plant responses to CO_2: Background and perspectives. – Plant Cell Physiol. **55**: 237-240, 2014.
Turano F.J., Dashnerm R., Upadhyaya A., Caldwell C.R.: Purification of mitochondrial glutamate dehydrogenase from dark-grown soybean seedlings. – Plant Physiol. **112**: 1357-1364, 1996.
Velikova V., Yordanov I., Edreva A.: Oxidative stress and some antioxidant system in acid rain-treated bean plants: protective role of exogenous polyamines. – Plant Sci. **151**: 59-66, 2000.
Wallsgrove R.V., Keys A.J., Lea P.J., Miflin B.J.: Photosynthesis, photorespiration and nitrogen metabolism. – Plant Cell Environ. **6**: 301-309, 1983.
Wu C., Sun Y., Yang G. *et al*.: Natural variation in stress response induced by low CO_2 in *Arabidopsis thaliana*. – Open Life Sci. **15**: 923-938, 2020.
Ye J.Y., Tian W.H., Jin C.W.: Nitrogen in plants: from nutrition to the modulation of abiotic stress adaptation. – Stress Biol. **2**: 4, 2022.
Zhang G., Tanakamaru K., Abe J., Morita S.: Influence of waterlogging on some antioxidative enzymatic activities of two barley genotypes differing in anoxia tolerance. – Acta Physiol. Plant. **29**: 171-176, 2007.
Zhang Y.H., Zhang G., Liu L.Y. *et al*.: The role of calcium in regulating alginate-derived oligosaccharides in nitrogen metabolism of *Brassica campestris* L. var. Tsen et Lee. – J. Plant Growth Regul. **64**: 193-202, 2011.
Ziegler C., Feraud M., Jouglet T. *et al*.: Regulation of promoter activity of ferredoxin-dependent glutamate synthase. – Plant Physiol. Bioch. **41**: 649-655, 2003.
Zivcak M., Brestic M., Balatova Z. *et al.*: Photosynthetic electron transport and specific photoprotective responses in wheat leaves under drought stress. – Photosynth. Res. **117**: 529-546, 2013.